



**HAL**  
open science

## Impact of amorphisation methods on the physico-chemical properties of amorphous lactulose

Frederic Ngono, Jean-François Willart, Gabriel J. Cuello, Monica Jimenez-Ruiz, Cherifa-Mounira Hamoudi-Ben Yelles, Frederic Affouard

### ► To cite this version:

Frederic Ngono, Jean-François Willart, Gabriel J. Cuello, Monica Jimenez-Ruiz, Cherifa-Mounira Hamoudi-Ben Yelles, et al.. Impact of amorphisation methods on the physico-chemical properties of amorphous lactulose. *Molecular Pharmaceutics*, 2020, 17, pp.1-9. 10.1021/acs.molpharmaceut.9b00740 . hal-02353960v1

**HAL Id: hal-02353960**

**<https://hal.univ-lille.fr/hal-02353960v1>**

Submitted on 25 Nov 2020 (v1), last revised 3 Mar 2021 (v3)

**HAL** is a multi-disciplinary open access archive for the deposit and dissemination of scientific research documents, whether they are published or not. The documents may come from teaching and research institutions in France or abroad, or from public or private research centers.

L'archive ouverte pluridisciplinaire **HAL**, est destinée au dépôt et à la diffusion de documents scientifiques de niveau recherche, publiés ou non, émanant des établissements d'enseignement et de recherche français ou étrangers, des laboratoires publics ou privés.

# Impact of amorphisation methods on the physico-chemical properties of amorphous lactulose

Frederic Ngono<sup>1,2</sup>, Jean-Francois Willart<sup>1,\*</sup>, Gabriel Julio Cuello<sup>2</sup>, Monica Jimenez-Ruiz<sup>2</sup>, Cherifa-Mounira Hamoudi-Ben Yelles<sup>3</sup>, Frederic Affouard<sup>1</sup>

<sup>1</sup>Univ. Lille, CNRS, INRA, ENSCL, UMR 8207 - UMET - Unité Matériaux et Transformations, F-59000 Lille, France

<sup>2</sup>Institut Laue Langevin, 71 Av. des Martyrs, CS 20156, F-38042, Grenoble, France

<sup>3</sup>Univ. Lille, Inserm, CHU Lille, U1008 - Controlled Drug Delivery Systems and Biomaterials, F-59000 Lille, France

**Abstract:** The influence of the amorphisation technique on the physico-chemical properties of amorphous lactulose has been investigated. Four different amorphisation techniques have been used: quenching of the melt, milling, spray-drying and freeze-drying, and amorphous samples have been analysed by DSC, NMR, and powder X-ray diffraction. Special attention has been paid to the tautomeric composition and to the glass transition of amorphised materials. It has been found that the tautomeric composition of the starting physical state (crystal, liquid or solution) is preserved during the amorphisation process and has a strong repercussion on the glass transition of the material. The correlation between these two properties as well as the plasticizing effect of the different tautomers have been clarified by molecular dynamic simulations.

**Keywords:** mutarotation, amorphisation, milling, quenching melt, spray-drying, freeze-drying, molecular dynamics simulation, MDSC, NMR

\* Corresponding author at: Université Lille Nord de France, F-59655 Villeneuve d'Ascq, France.

E-mail address: jean-francois.willart@univ-lille.fr (J.F. Willart).

## 1. Introduction

Glass forming sugars play a major role in nature as they are able to protect biological systems from many external stresses<sup>1,2</sup>. They are in particular synthesised in large quantities by organisms which can resist to freezing, high temperatures and severe dehydrations<sup>2-4</sup>. Glass forming sugars are also widely used in pharmaceutical formulation<sup>5,6</sup> for the encapsulation, the stabilisation, and the release of drugs<sup>7,8</sup> and nutrients<sup>9</sup>. They help to preserve labile biological molecules like proteins from stresses induced by some usual pharmaceutical processes<sup>10,11</sup> (freeze-drying, spray-drying, milling, extrusion, heating...).

Most sugars can exist in different tautomeric forms which can adopt cyclic or open chain conformations<sup>12,13</sup>. This is, for instance, the case of glucose<sup>14</sup>, sorbose<sup>15</sup>, fructose<sup>16</sup>, lactose<sup>17</sup> and many others. Mutarotation is another striking feature of sugars<sup>15,18-21</sup> which is the conversion of one tautomeric form into another. The kinetic of this conversion strongly depends on the physical state of the material. In solution or in the liquid state, mutarotation is generally fast and an equilibrium tautomeric composition is rapidly reached. In the amorphous solid state, mutarotation has been found to require a much higher activation energy so that mutarotation kinetics are quite slower<sup>16,22-25</sup>. While there is almost no molecular mobility in crystals, Tombari et al. have postulated that mutarotation can also occur in this ordered physical form through the mediation of vacancies and defects. It then causes local amorphisations which could ultimately lead to the liquefaction of sugars well below their reputed melting points<sup>26</sup>. All these changes in the tautomeric composition due to mutarotation can have a strong repercussion on the physical properties of the material and in particular on its glass transition temperature (T<sub>g</sub>). For instance, Włodarczyk et al.<sup>16</sup> have shown that the T<sub>g</sub> of tautomerically pure fructose (pyranose form) can change by 10°C when it converts to a mixture of pyranose and furanose forms by mutarotation. Such a change of the molecular mobility can thus have critical repercussion on the physical stability of glass forming sugars.

In practice, amorphous sugars can be produced by many different techniques which drive materials through different intermediate physical states<sup>27</sup>. To cite only a few: i) the classical thermal quench of the melt involving the liquid state<sup>28,29</sup>, ii) the mechanical route (compression, milling) occurring entirely in the solid state<sup>30-32</sup> iii) the solvent removal processes (freeze-drying<sup>33</sup>, spray-drying<sup>34</sup>...) requiring the dissolution of the drug in a solvent. These different processes are not yet fully understood and can possibly lead to different amorphous states characterised by different chemical and physical properties. In particular, the amorphisation process can generate impurities arising from chemical degradation, leave residual traces of solvent, and modify the tautomeric composition if molecules are prone to mutarotation. It can also have an impact on the enthalpic level, the short-range order and the microstructure of the amorphous state. All these parameters must thus be understood and controlled as they have a direct influence on the glass transition and the effective physical stability of the final product against recrystallisation.

In this paper, we investigate the influence of the amorphisation route on the physical and chemical states of amorphous lactulose<sup>35</sup>. Four amorphisation routes were explored: quenching of the melt, milling of the crystal, spray-drying and freeze-drying. Physical and chemical properties of these samples were investigated by nuclear magnetic resonance

(NMR), differential scanning calorimetry (DSC) and X-ray diffraction (XRD). Lactulose was chosen for its excellent glass forming ability, its high solubility and its complex tautomerism made of five tautomers which can inter convert by mutarotation<sup>36</sup>. Tautomers A (galactosyl  $\beta$ -furanose), B (galactosyl  $\alpha$ -furanose) and C (galactosyl  $\beta$ -pyranose) were detected in large proportions. Their chemical structures are reported in Figure 1. On the contrary, tautomers D (galactosyl  $\alpha$ -pyranose) and E (partially open-chain transiently produced during mutarotation) are much rarer and have not been detected in the present study.

Special attention has been paid here to the effect of the amorphisation process on the tautomeric compositions of the resulting amorphous state and to its repercussion on the glass transition temperature ( $T_g$ ). The correlation between these two characters as well as the plasticizing effect of the different tautomers have been further investigated by molecular dynamic (MD) simulations.

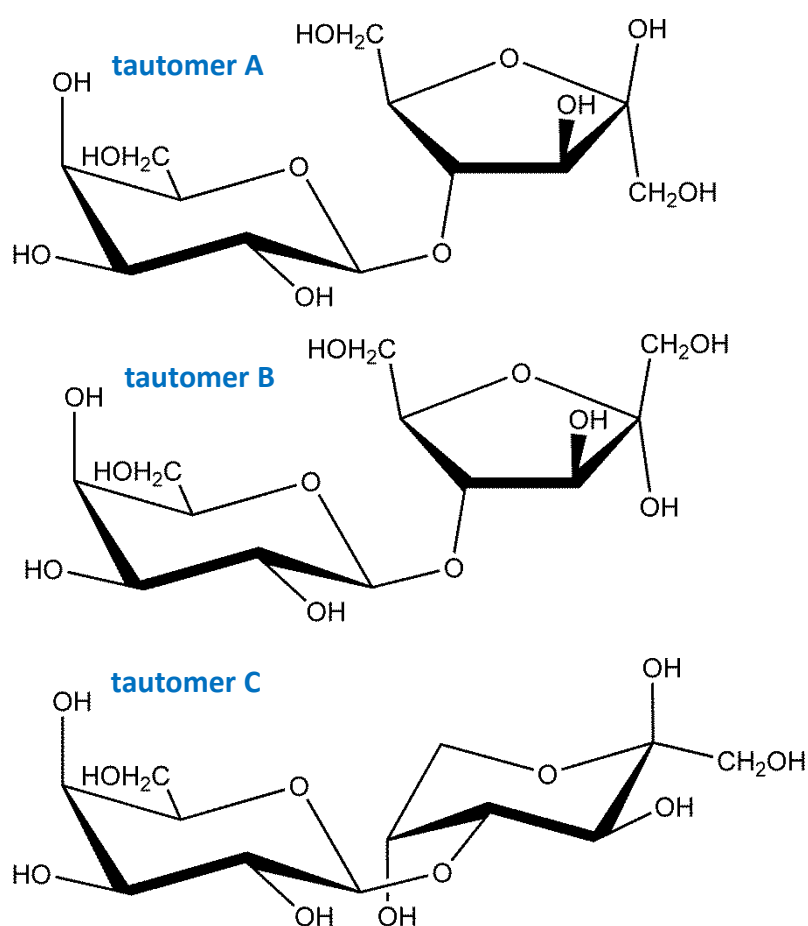


**Figure 1:** Chemical structures of the three main disaccharide lactulose ( $C_{12}H_{22}O_{11}$ ) tautomers A, B and C. There exists two other tautomers that appear only in the state of traces<sup>36</sup>.

## 2. Experimental and simulations

### 2.1 Material

Crystalline anhydrous lactulose was purchased from Sigma Aldrich. Thermogravimetric experiments have shown that it contains about 3.5 % of water inclusions. The commercial form was thus slightly crushed to favour water release, and dried at 70 °C during 15 min. The obtained sample has been checked to be totally crystalline, and has been used for the different experiments.

### 2.2 Amorphisation methods

We used four different techniques to prepare amorphous lactulose compounds: quenching of the melt, milling, spray-drying and freeze-drying. The amorphous samples obtained using these techniques will be respectively noted QM, MIL, SD and FD in the following.

#### a- Quenching of the melt

Quenched melt was obtained by heating (5°C/min) crystalline lactulose just above its melting point ( $T_m = 161^\circ\text{C}$ ) and by quenching (10°C/min) the melt at 20°C. The whole process was performed in the DSC device, under a nitrogen atmosphere and with a small sample size. This allows to control the melting process and to minimise the time spent above  $T_m$  in order to limit as much as possible thermal degradation<sup>37</sup>.

#### b- Milling

Ball milling was performed during 8h in a cold room at -10°C and under a dry atmosphere (RH ~ 0%) using a high-energy planetary mill (Pulverisette 7—Fritsch, Idar-Oberstein, Germany). We used ZrO<sub>2</sub> milling jars of 43 cm<sup>3</sup> with seven balls ( $\phi = 15$  mm) of the same material. 1 g of material was placed in the milling jar corresponding to a ball/sample weight ratio of 75:1. The rotation speed of the solar disk was set to 400 rpm. We took care to alternate milling periods (typically 10 min) with pause periods (typically 5 min) in order to limit the mechanical heating of the sample. Lactulose was milled during 8h as this milling time was reported to be long enough to induce a complete amorphisation<sup>37</sup>.

#### c- Spray-drying

Lactulose was dissolved in distilled water (5 g / 50 ml) at room temperature (RT) and spray-dried using a Buchi B-290 mini spray dryer (Buchi, Basel, Switzerland), equipped with a 0.7 mm nozzle (feed rate: 5 mL/min; air flow rate: 601 l/h; inlet temperature: 120°C± 2°C; outlet temperature: 70± 5°C; concurrent feed flow/inlet drying gas-nitrogen).

#### d- Freeze-drying

Lactulose was dissolved in distilled water (5 g / 50 ml) at RT and freeze-dried using the freeze dryer Christ Epsilon 2-4 LSC (Martin Christ, Osterode, Germany): freezing at  $-45\text{ }^{\circ}\text{C}$  for 4 h, primary drying at  $-20\text{ }^{\circ}\text{C}/0.007\text{ mbar}$  for 20 h, and secondary drying at  $+35\text{ }^{\circ}\text{C}/0.0014\text{ mbar}$  for 40 h.

### 2.3 DSC experiments

Differential Scanning Calorimetry (DSC) was performed with the DSC Discovery of TA Instruments. For all experiments, the sample was placed in an open aluminum pan (container with no cover) to allow any residual free water to be removed upon heating, and was flushed with highly pure nitrogen gas. Temperature and enthalpy readings were calibrated using pure indium at the same scan rates and with the same kind of pans used in the experiments. Experiments were performed in the temperature modulated mode (MDSC) using a heating rate of  $5\text{ }^{\circ}\text{C}/\text{min}$ , a modulation amplitude of  $0.663\text{ }^{\circ}\text{C}$  and a modulation period of 50 s. These parameters correspond to “heat only” conditions.

### 2.4 X-ray diffraction experiments

X-ray diffraction (XRD) experiments were performed with a PanAlytical X’PERT PRO MPD (Almelo, The Netherlands) diffractometer ( $\lambda_{\text{CuK}\alpha} = 1.5418\text{ \AA}$  for combined  $\text{K}\alpha_1$  and  $\text{K}\alpha_2$ ) equipped with an X’celerator detector (Almelo, The Netherlands). Samples were placed into Lindemann glass capillaries ( $\phi = 0.7\text{ mm}$ ). Data were recorded from  $5^{\circ}$  to  $40^{\circ} 2\theta$  by step of  $0.0167^{\circ} 2\theta$  using a counting time of 50 s every  $2^{\circ} 2\theta$ .

### 2.5 NMR experiments

NMR spectra were recorded with the NMR 400 MHz spectrometer commercialised by Bruker. 10 mg of sample were dissolved into 0.75ml of Dimethyl Sulfoxide (DMSO). We used this solvent for its ability to slowdown the mutarotation in solution strongly<sup>38,39</sup>. The signal was collected at RT just after (typically 3 min) the dissolution, in order to limit as much as possible the mutarotation. For all experiments we used a 5 mm TBI probe which is suitable for proton NMR. Results were analysed using the TopSpin 3.5pl5 software of Bruker.

### 2.6 MD simulations

We have performed molecular dynamics (MD) simulations using the DLPOLY package<sup>40</sup> (version 4.07) and the OPLS (Optimised Potentials for Liquid Simulations) force field<sup>41,42</sup>. We chose this force field due to its capability of reproducing successfully the experimental data for a large number of molecules with low molecular weight<sup>43–45</sup>. We conducted the simulations either in the NPT or the NVT statistical ensemble, with  $N$  the number of molecules,  $P$  the pressure,  $T$  the temperature, and  $V$  the volume. The number of molecules,  $N$ , was fixed in the simulations. The pressure and temperature were controlled with a Nose-Hoover barostat and thermostat, with relaxation times of 2.0 ps and 0.2 ps respectively. We

performed all NPT simulations at atmospheric pressure and we used the equilibrated volume at a given  $P$  and  $T$  for subsequent NVT simulations. The time step to integrate Newton's equation of motion was chosen as 0.001 ps. A cut-off radius of 10 Å was used to calculate short-range van der Waals interactions. Long-range electrostatic forces were calculated using a shifted Coulombic potential, with the same cut-off radius. Periodic boundary conditions were applied in all directions.

In order to investigate the impact of the tautomeric composition on the molecular mobility of amorphous lactulose, we have calculated the diffusion coefficients of tautomers A and C, as well as their gyration radii  $R_g$ . The diffusion coefficient  $D$  is determined from the long-term evolution of the mean square displacement ( $\langle r^2(t) \rangle \sim 6Dt$ ). The gyration radius  $R_g$  is determined thanks to the following equation:

$$R_g = \langle (\sum_{\alpha} m_{\alpha} s_{\alpha}^2 / \sum_{\alpha} m_{\alpha})^{1/2} \rangle \quad \text{Eq. 1}$$

where  $m_{\alpha}$  is the mass of the  $\alpha$  atom, located at a distance  $s_{\alpha}$  from the molecule centre of mass,  $\langle \rangle$  indicates an average over the  $N$  molecules and time.

We have also calculated the number of intramolecular and intermolecular hydrogen bonds (HBs) developed by each tautomer. To do so, we have considered that an HB exists if the oxygen–oxygen distance  $d(\text{O-O})$  is smaller than 3.4 Å and the O-H...O angle is larger than 150.0°. This geometric criterion includes only well-formed and strong HBs<sup>46,47</sup>. It should be noted that use of less stringent criteria ( $d(\text{O-O}) < 4.0$  Å, and O-H...O angle  $> 120^\circ$ ) including quite deformed and weaker HBs have given similar results. All those results are given in Supporting Information.

Two amorphous systems respectively composed of only tautomer A and only tautomer C have been investigated from MD simulations. Each simulation box was generated using the same procedure. First, we build an initial cubic pseudo-crystal box composed of 64 molecules. Then, it was melted at a high temperature of 700K during 2ns in the NPT ensemble in order to eliminate any orientational or translational order, and to thus obtain a fully disordered system in the liquid state. Finally, we hyper-quenched the liquid box from 700 K to 300 K at a cooling rate of 10K/100ps. We applied a further equilibration of 8 ns (including 6 ns in the NPT ensemble and 2 ns in the NVT ensemble) to the resulting boxes at 650K, 600K, 550K and 500K. After equilibrations, several MD trajectories of different lengths (see Table 1) were generated at the different temperatures and used to calculate the diffusion coefficients, as well as the gyration radii. The densities of the different boxes are also reported in Table 1.

**Table 1:** Densities and lengths of the MD trajectories generated at the different temperatures from both systems.

Temperature (K)	Density ( $\pm 0.01$ g/cm <sup>3</sup> )		Simulation time (ns)	
	tautomer A	tautomer C	tautomer A	tautomer C
650	1.29	1.30	20	20
600	1.33	1.35	20	20
550	1.37	1.39	150	150
500	1.41	1.42	150	200

### 3. Results and discussion

#### 3.1. Structure of processed materials

Figure 2 shows the X-ray diffraction (XRD) patterns of crystalline lactulose recorded at RT after different processing: quenching of the melt (QM), milling (MIL), spray-drying (SD) and freeze-drying (FD). Clearly, the four diffraction patterns are free of Bragg peaks which indicates that each process has produced amorphous lactulose. Moreover, the four patterns appear to be very similar, showing a diffusion halo centred around  $2\theta = 18^\circ$ . Structural differences between the four amorphous states, if any, are too small to be detected by classical X-ray diffraction. However, it is worth noticing that subtle structural differences between the different amorphous states have been detected by neutron diffraction investigations. These results are reported in details in Ref<sup>48</sup>.

The physical stability of SD, FD, MIL and QM amorphous samples was tested through long annealing at different temperatures. At 20°C, the amorphous samples were found to be stable during 6 months, except the MIL sample which showed slight signs of recrystallisation through the development of tiny Bragg peaks. For higher annealing temperatures, chemical degradation was found to occur before any crystallisation could be observed.

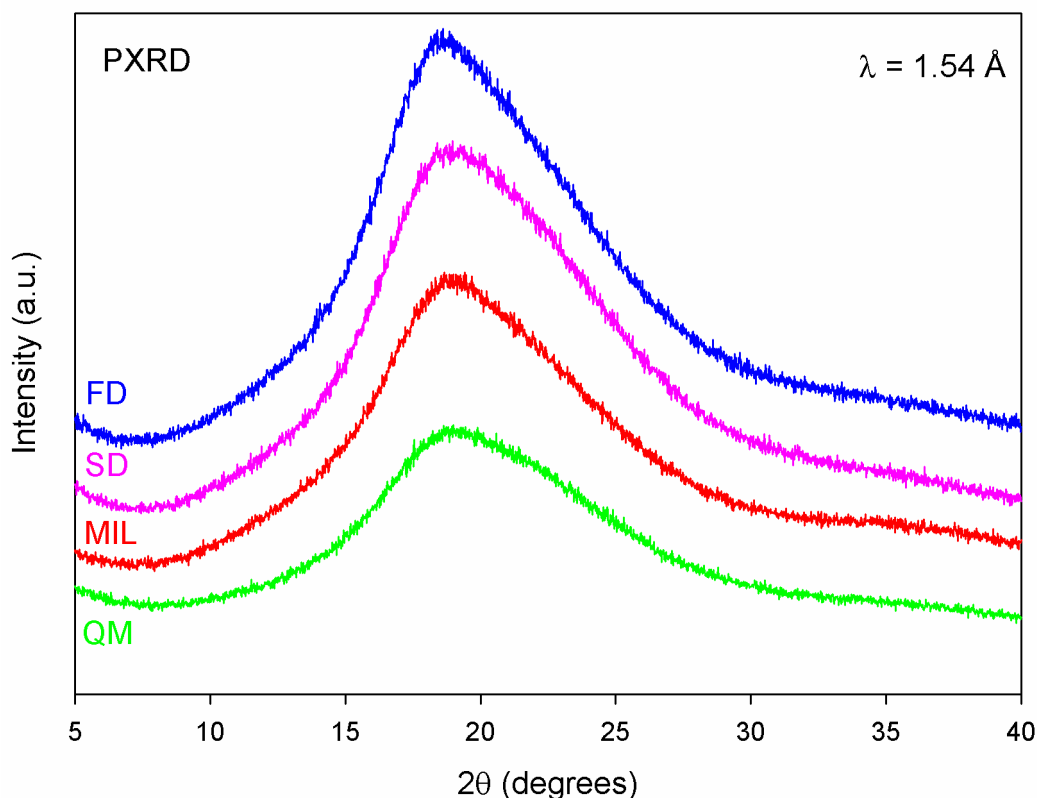


**Figure 2:** XRD patterns of amorphous lactulose samples: FD (blue line), SD (pink line), MIL (red line) and QM (green line).

### 3.2. Tautomeric composition of processed materials

Figure 3 shows NMR spectra of crystalline lactulose recorded after the four amorphisation processes: milling (MIL), freeze drying (FD), spray drying (SD), and quenching of the melt (QM). The unprocessed crystal is also reported for comparison. In each case the NMR spectrum was recorded within three minutes after dissolution in DMSO to limit as much as possible any mutarotation due to the dissolution itself. The validity of this protocol is demonstrated in Supporting Information. All spectra show three well defined peaks between 5.2 ppm and 5.7 ppm which are characteristic of tautomers A (5.35 ppm), B (5.66 ppm) and C (5.28 ppm). We can also note strong differences in the relative intensity of the peaks from one sample to another, indicating noticeable differences in the tautomeric composition of the samples. The tautomeric compositions obtained by integration of the peaks are reported in Table 2. It is worth mentioning that the characteristic peaks were assigned on the base of previous studies<sup>36,39,49</sup>.

In the unprocessed crystal the tautomeric composition appears to be  $X_A = 79 \pm 4\%$ ,  $X_C = 10 \pm 4\%$  and  $X_B = 11 \pm 4\%$ . These values are slightly different from those previously obtained by Jeffrey et al.<sup>36</sup> ( $X_A = 74\%$ ,  $X_B = 10\%$  and  $X_C = 15\%$ ). However, we have found that the tautomeric compositions can noticeably vary from one batch to another. In particular,  $X_A$  and  $X_C$  vary respectively in the ranges [74% , 79%] and [10% , 16%] while  $X_B$  is almost constant. Variations of  $X_A$  and  $X_C$  are probably due to the experimental conditions used by the provider to produce the crystalline lactulose.

The tautomeric composition of the QM is different from that of the crystal. In particular,  $X_A$  (49%) decreases to the benefit of  $X_C$  (34%) and  $X_B$  (17%). These changes reveal a strong mutarotation occurring upon melting. Moreover, the QM spectrum shows some additional small peaks which are likely to result from some thermal degradation occurring during melting<sup>37</sup>.

The tautomeric composition ( $X_A = 82\%$ ,  $X_B = 8\%$  and  $X_C = 10\%$ ) of the sample milled during 8h under a dry atmosphere (RH ~0%) appears to be very close to that of the initial crystalline form. This means that the amorphisation induced by milling has occurred without any mutarotation. Such a behaviour was already reported for lactose<sup>50</sup> and glucose<sup>51</sup>. It proves that the amorphisation induced by milling really occurs in the solid state and that the sample temperature never exceeds, even locally, the melting point which would inevitably lead to a strong mutarotation as found for the QM sample. The absence of melting during milling is also proved by the absence of thermal degradation in the NMR spectrum which is characteristic of amorphous lactulose produced by QM. It must also be noted that if the milling is performed under a non-dried atmosphere, a noticeable mutarotation is observed. In that case, the mutarotation is mediated by the free water caught during the milling so that the tautomeric composition converges towards that characteristic of lactulose dissolved into water.

The tautomeric compositions of SD and FD samples are similar to each other, but noticeably different from those of the other compounds. Tautomer C predominates in SD and FD compounds, while tautomer A predominates in the other amorphous samples. These differences of tautomeric compositions are likely to be due to the fact that SD and FD processes require an initial dissolution stage of lactulose. Mayer et al.<sup>49</sup> have determined the tautomeric composition of lactulose in solution in water at RT. This composition is reported in Table 2 and appears to be very close to that those of SD and FD samples. This suggests that removal of water occurring during SD and FD processes occurs with almost no mutarotation. In the case of freeze-drying the mutarotation is likely to be blocked because the water removal occurs in the solid state where the molecular mobility is almost non-existent. In the case of spray-drying the removal of water molecules occurs on a very short time scale which does not allow mutarotation to occur. As a result, the tautomeric composition of lactulose in solution is preserved in the SD and FD samples.

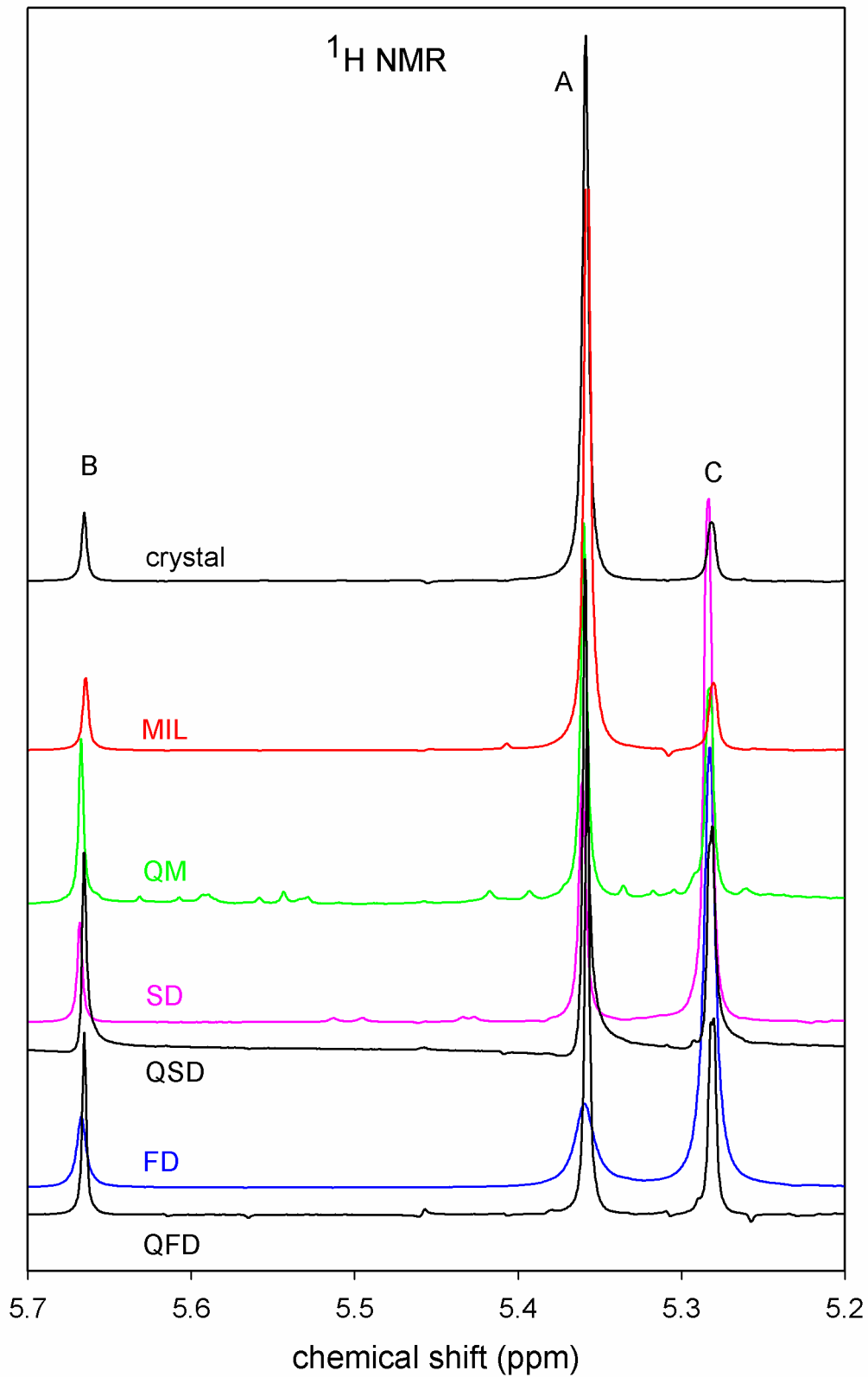


**Figure 3:** NMR spectra of different lactulose samples. From top to bottom: crystal (black line), MIL (red line), QM (green line), SD (pink line), QSD (black line), FD (blue line), QFD (black line).

**Table 2:** Tautomeric compositions and glass transition temperatures of different lactulose samples. The tautomeric composition of lactulose in solution in water<sup>49</sup> is also reported for comparison.

Samples	tautomer A in % ( $\pm 4$ )	tautomer B in % ( $\pm 4$ )	tautomer C in % ( $\pm 4$ )	T <sub>g</sub> (°C) ( $\pm 1$ )
crystal	79	11	10	---
MIL at RH#0	82	8	10	88
In solution [Mayer] <sup>49</sup>	24	11	65	---
QM	49	17	34	99
SD	29	9	62	98
QSD	50	18	32	88
FD	24	8	68	98
QFD	51	18	31	88

### 3.3. Glass transition of processed materials

Figure 4 shows the MDSC heating scans (reversible signals) of lactulose amorphised by the different techniques (quenching of the melt, milling, spray-drying and freeze-drying). All of them show a Cp jump characteristic of a glass transition that confirms their amorphous character. Moreover, no sign of exothermic crystallisation could be detected in the total heat flow upon heating (5°C/min) revealing the high physical stability of each amorphous lactulose sample. It must be noted that for the MIL, SD and FD samples the Cp jump occurs in two steps. The first step corresponds to the glass transition itself while the second step is an artefact which is frequently observed in amorphous materials having a complex microstructure<sup>52</sup>. MIL and SD materials are finely divided powders and FD materials are characterised by a high porosity. Both kinds of microstructure have generally a much lower thermal conductivity than bulk amorphous materials obtained by QM giving rise to an apparent lower Cp. Above T<sub>g</sub>, the viscosity drops, so that the previous microstructures collapse giving rise to dense droplets of liquid which have a much better thermal conductivity. As a result, the apparent specific heat increases giving rise to the second Cp jump in runs 2, 3 and 4. The glass transition temperatures of the four amorphous lactulose samples, derived from the first Cp jumps, are reported in Table 2. They appear to depend noticeably on the amorphisation technique, ranging from 88°C for the MIL to 99°C for the QM. We show hereafter that this variable T<sub>g</sub> is due to chemical changes arising either from thermal degradation or from mutarotation.

Recently, it was reported that the chemical degradation of lactulose on approaching the melting point has a noticeable effect on the glass transition temperature of the quenched melt<sup>37</sup>. It was shown in particular that the degradation products have an anti-plasticizing effect, increasing the apparent T<sub>g</sub> of the amorphous material. Different melting protocol can

thus give rise to slightly different  $T_g$ , as it has been observed for several compounds<sup>35,53</sup>. We have taken advantage of the possibility to obtain non degraded amorphous lactulose by SD and FD to produce quenched liquid lactulose without any thermal degradation. This was done by heating (5°C/min) the SD and FD samples up to 150°C. This temperature is located sufficiently above  $T_g$  in order to have the liquid state (although metastable), and sufficiently below the melting point ( $T_m = 162^\circ\text{C}$ ) to avoid any chemical degradation<sup>37</sup>. The metastable liquids thus obtained have then been quenched to 20°C to form non degraded quenched liquids called QSD (Quenched Spray Dried) and QFD (Quenched Freeze Dried). The NMR spectra of these quenched liquids are reported in figure 3. They do not show the degradations spikes previously detected in the QM sample which proves that QSD and QFD are not chemically degraded. The calculated tautomeric compositions derived from the two spectra are reported in Table 2. It appears that both of them are very close to the tautomeric composition of the QM sample. This means that a strong mutarotation has occurred in the SD and FD samples during their small excursion above  $T_g$ , to reach that of the liquid state. The heating DSC scans of the QSD and QFD samples are reported in figure 4 (runs 5 and 6). They both show three interesting features:

- (i) A well-defined glass transition at 88°C occurring through a single  $C_p$  jump. Such a single  $C_p$  jump indicates that the complex microstructures characteristic of the SD and FD samples have been erased above  $T_g$  and replaced by a droplet microstructure typical of quenched melts.
- (ii) The glass transition is noticeably depressed compared to those of SD and FD lactulose. This shift must thus clearly be attributed to the changes in the tautomeric composition previously detected (Table 2).
- (iii) The glass transition of QSD and QFD are also strongly depressed compared to that of the QM, while the three amorphous samples have very close tautomeric compositions. This confirms that the highest glass transition of the QM is due to an anti-plasticization effect arising from degradation products.

The above results indicate that the glass transition temperature of amorphous lactulose depends noticeably on its tautomeric composition. In particular, the analysis of Table 2 shows that the samples rich in pyranose moiety (SD and FD) have a glass transition temperature 10 °C higher than that of samples rich in furanose moiety (QSD and QFD). This suggests that tautomer A has a plasticizing effect on the tautomeric mixture while tautomer C has an anti-plasticizing effect. These behaviours are coherent with those previously detected on fructose by Włodarczyk et al.<sup>16</sup> using Dielectric Spectroscopy. These authors have shown that mutarotation can change the  $T_g$  of fructose by 10°C and that the  $T_g$  of the pyranose moiety is higher than the furanose one. Moreover, the variation of  $T_g$  with changes in the tautomeric composition due to solid state mutarotation is not specific to sugars. It was also noticed in some drugs like glibenclamide<sup>54</sup> and aberchrome 670<sup>55</sup>, and in some polymers like azopolymers (polymers containing azobenzene) where mutarotation (photo-isomerization) can be interestingly triggered by UV irradiation<sup>56</sup>. All these materials have thus the interesting property to have a tunable  $T_g$  which can be varied by some external physical parameters.

In the case of lactulose, a better characterisation of the effect of each tautomer on  $T_g$  can hardly be achieved experimentally. The difficulty mainly arises from the impossibility to control the tautomeric composition of amorphous lactulose and to produce amorphous lactulose tautomericly pure. In the next section, we show how numerical simulations can overcome these experimental limitations and give interesting information on the influence of the tautomers (A and C) on the glass transition.

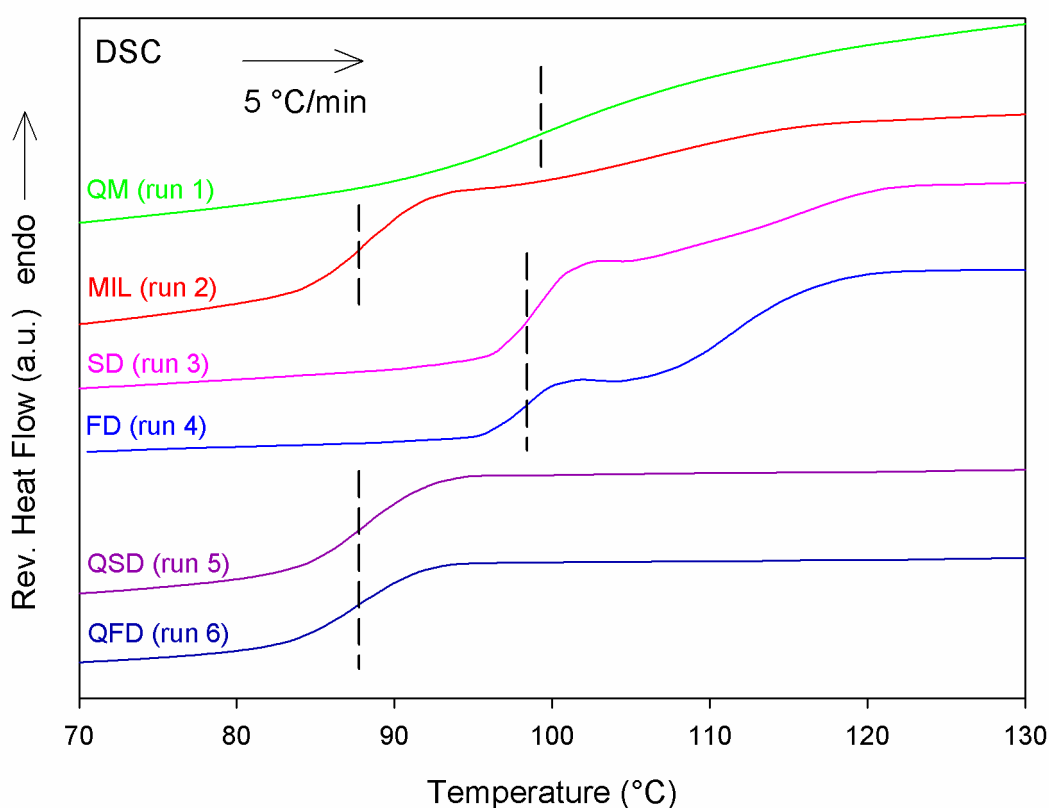


**Figure 4:** Heating MDSC curves (5 °C/min) of amorphous lactulose samples. From top to bottom: QM (green line), MIL (red line), SD (pink line), FD (blue line), QSD (purple line) and QFD (dark blue line). For reason of clarity, only the reversible signals are represented. The dashed lines mark the position of the glass transition temperature.

### 3.4. Study of the molecular mobility of tautomers A and C by MD simulations

Molecular mobility of amorphous compounds composed only of tautomer A, and only of tautomer C was studied by MD simulations in order to understand better the differences found concerning the glass transition of the different processed amorphous samples and their link with the tautomeric fractions. The glass transition temperature could be determined by MD simulations from the temperature dependence of the density<sup>57,58</sup>. Assuming a linear evolution of the density as function of the temperature at very low and very high temperatures, the crossing between the high temperature equilibrium line and the low temperature out of

equilibrium line can usually provide a rough estimation of the glass transition temperature. However, very high cooling rates are used in MD simulations ( $\sim 10^{12}$  K/min) compared to experimental cooling rates ( $\sim 10$  K/min) which usually lead to an overestimation of  $T_g$  of about 100K in some cases and therefore to high discrepancies<sup>59</sup>.

Instead of determining  $T_g$ , the molecular mobility of tautomers A and C was studied separately by means of their diffusion coefficient  $D$  obtained from the mean-squared displacement (msd) calculated in the liquid state from fully equilibrated MD runs. Since lactulose is a quite viscous liquid on the MD timescales, the diffusive regime can be reached only at relatively high temperatures.

It is worth mentioning that in this work, we have assumed that molecular mobility (as probed by the diffusivity) should have a monotonous behaviour as function of the tautomeric concentration in a mixture. Indeed, since the tautomers A, B and C are similar molecules, they are not expected to develop strong interactions in a mixture, and the  $T_g$  of the lactulose tautomeric mixture should obey the Gordon-Taylor law<sup>60</sup> (with  $K$  close to 1) as observed for some other mixtures (lactose/budesonide, lactose/mannitol)<sup>61</sup>. Therefore, the determination of molecular mobility of liquids composed of single tautomers should allow to understand  $T_g$  differences of mixture observed experimentally.

Figure 5 shows the diffusion coefficients calculated at 500, 550, 600 and 650 K in lactulose boxes having only tautomer A (green line) and only tautomer C (blue line). The obtained values are also reported in Table 3. In the studied temperature range, tautomer A is clearly found more diffusive than tautomer C. Upon decreasing temperature, the difference between the diffusion constant of the tautomers A and C also tends to increase. It suggests that a liquid composed of only tautomers A would possess a lower glass transition temperature than a liquid composed of only tautomers C. It should be noted that this trend is consistent with the results obtained with other time-dependent function such as the coherent intermediate scattering function  $S(Q,t)$  of the two tautomers (data not shown here). Therefore, a mixture composed of a higher proportion of tautomer C, as found for the SD lactulose (%A = 29, %C = 62) and the FD lactulose (%A = 24, %C = 68), could be expected to have a higher  $T_g$  than a mixture composed of a higher proportion of tautomer A, as found for the MIL lactulose (%A = 82, %C = 10). It is worth mentioning that extrapolation of the diffusion coefficient to  $D \approx 10^{-20}$  m<sup>2</sup>/s using a MYEGA law<sup>62</sup> shows that the simulated glass transition of the pure tautomer C liquid would be approximately 20K higher than the one of the pure tautomer A liquid. This result is compatible with the experimental  $T_g$  obtained on the different compounds. It should also be mentioned that the same calculations have been performed for tautomer B, and the results clearly show that tautomers A and B have the same molecular mobility and diffusivity. Therefore, two main behaviours exist in the different amorphous lactulose compounds: tautomers A and B on the one hand, and tautomer C on the other hand.

The difference in diffusivity between both tautomers A and C can be understood from the difference of the densities reported in Table 1. Indeed, a liquid composed of only tautomers C always seems a bit denser than a liquid composed of only tautomers A. However, this difference is very small about 0.01 or 0.02 g/cm<sup>3</sup> and thus of the same order of the uncertainties  $\pm 0.01$  g/cm<sup>3</sup>. Moreover, differences in transport properties of fructose (five-membered ring) and glucose (six-membered ring) have been observed experimentally<sup>63</sup>, and are well in line with our results. In order to understand better the origin of the molecular mobility difference between tautomers A and C, the distribution of their gyration radii at the different investigated temperatures have been computed. The obtained results at T = 500 K are represented in the inset of Figure 5. As it can be seen, the maximum of the distribution is at slightly higher position for tautomer C compared to tautomer A. In addition, at high gyration radius values, the amplitude of the distributions is higher for the case of tautomer C compared to tautomer A. Same behaviour is also found at 550, 600 and 650 K. All these results indicate that tautomer C would possess a size slightly larger than tautomer A. This difference is particularly well in line with the differences in topology between tautomer C composed of two six-membered rings on the one hand and tautomer A composed of one five-membered and one six-membered ring on the other hand (see Figure 1). Assuming that smaller molecules diffuse faster than larger molecules and vice-versa, this would explain the molecular mobility difference observed between tautomer A and C.

Surprisingly, tautomer C develops less intermolecular hydrogen bonds (HBs) than tautomer A at all temperatures (see Supporting Information) despite its lower diffusivity. Indeed, we could have expected a higher number of HBs for tautomer C. For two other disaccharides, namely trehalose and sucrose, results shown that trehalose molecules develop more intermolecular HBs than sucrose molecules<sup>47</sup>, with a higher glass transition temperature (lower diffusivity) for trehalose:  $T_g(\text{trehalose})^{64} = 120^\circ\text{C}$  ;  $T_g(\text{sucrose})^{65} = 69^\circ\text{C}$ .

At 500K for example, tautomer A develops about  $6.4 \pm 0.2$  intermolecular HBs while tautomer C develops about  $5.8 \pm 0.2$  intermolecular HBs. Almost no intramolecular (between rings) HBs were developed by each tautomer: about  $0.1 \pm 0.1$  for tautomer A, and  $0.3 \pm 0.1$  for tautomer C were calculated. A thorough analysis of the intermolecular HBs allows us to understand the observed differences. Indeed, the oxygen atom of the CH<sub>2</sub>OH groups (three are present in tautomer A and two in tautomer C) develops between 1.2 and 1.6 HBs, with an average value of 1.44 for tautomer A and 1.40 for tautomer C. The oxygen atom of the OH groups not belonging directly to CH<sub>2</sub>OH groups (five are present in tautomer A and six in tautomer C) develops between 0.1 and 0.9 HB, with an average value of 0.49 for both tautomers. Clearly, the oxygen atom in the CH<sub>2</sub>OH groups always develops more HBs than in the OH groups. This result is expected since the rotation around the C-C bond is allowed, thus increasing the accessibility of the oxygen atom in the CH<sub>2</sub>OH group compared to the oxygen atom in the OH group. Therefore, the differences between intermolecular HBs developed by both tautomers are due to the fact that tautomer A has three CH<sub>2</sub>OH groups, while tautomer C has only two CH<sub>2</sub>OH groups (see Figure 1). It could be noted that tautomer A in the crystalline state<sup>36</sup> also form no intramolecular HB. This result gives confidence on the number of HBs calculated by MD simulations.

Our results thus suggest that HBs cannot be used to explain molecular mobility differences in this case. The HBs are not the only intermolecular interactions develop by the tautomers. Additional interactions, such as hydrophobic C-C ones, might also impact the molecular mobility of the tautomers. The overall intermolecular interaction energy of both tautomers should be calculated to check this assumption.

**Table 3:** Diffusion coefficients of tautomers A and C at different temperatures. The uncertainties on those values are very small and have not been reported.

Temperature (K)	Diffusion coefficients ( $\times 10^{-9} \text{ m}^2/\text{s}$ )	
	Tautomer A	Tautomer C
650	19.581	13.731
600	5.3082	3.7256
550	1.2750	0.4711
500	0.073108	0.015084

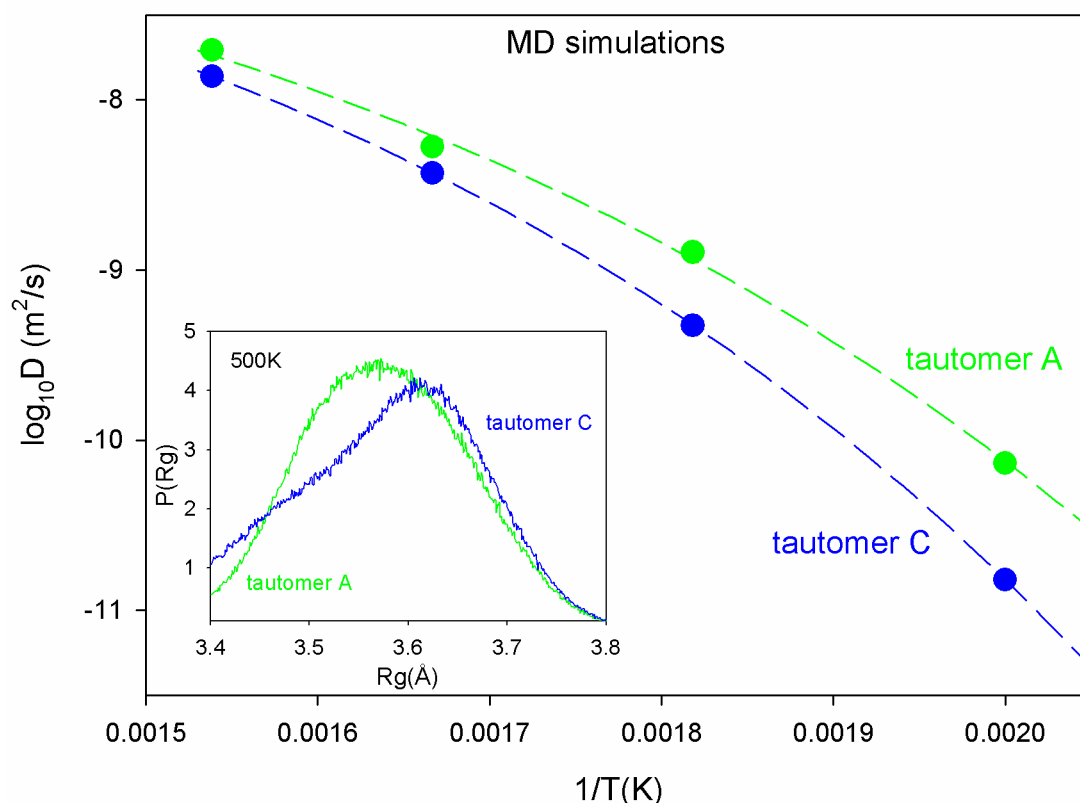


**Figure 5:** Diffusion coefficients of tautomers A (green points) and C (blue points) as a function of the temperature. The data are fitted with a MYEGA law<sup>62</sup>. Diffusion coefficients of tautomer B (not shown) are very similar to tautomer A. The inset shows the distribution of

the gyration radii of tautomers A (green line) and C (blue line) calculated at 500K. Same behaviour is also found at 550, 600 and 650 K.

## 4. Conclusion

In this paper, we have investigated the influence of the amorphisation route on the physical and chemical properties of amorphous lactulose. Four amorphisation routes have been explored: quenching of the melt, high energy milling, freeze drying and spray drying. Special attention has been paid to the tautomeric composition and to its influence on the glass transition temperature. It appears that the tautomeric composition of each amorphous state reflects that of the physical state preceding the amorphisation process. In particular, the tautomeric composition is that of the liquid state for the quenched liquid, that of the crystal for the milling induced amorphous sample and that of lactulose in solution for the spray-dried and freeze-dried samples. The different tautomeric compositions have been found to have a noticeable repercussion on the glass transition which can vary in the range [88°C; 99°C]. The results also indicate that tautomer A has a plasticizing effect on the tautomer mixture while tautomer C has an anti-plasticizing effect. Molecular dynamic simulations have confirmed this point and have shown that the molecular size could be responsible of this difference of mobility between the tautomers.

## Acknowledgment

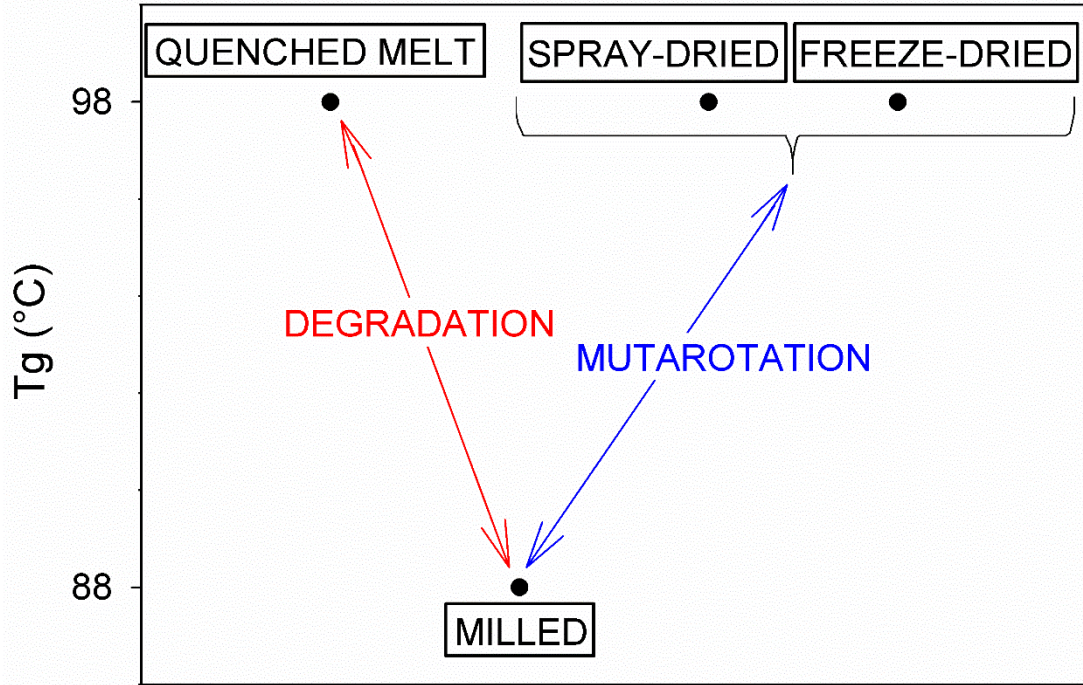
This project has received funding from the Interreg 2 Seas programme 2014-2020 co-funded by the European Regional Development Fund under subsidy contract 2S01-059\_IMODE.

F. NGONO thanks the ILL PhD program and the University of Lille for their financial support.

We thank very much Dr. Adrien Lerbret for all the fruitful discussions.

**Supporting Information Available:** Two sections are presented. The first one shows ability of DMSO to slow down mutarotation in lactulose. The second one shows the number of intermolecular and intramolecular HBs developed by tautomers A and C at different temperatures, using four different geometric criteria to determine the HBs:  $d(\text{O}\dots\text{O}) < 3.4 \text{ \AA}$  and  $(\text{O-H}\dots\text{O}) > 120^\circ$ ;  $d(\text{O}\dots\text{O}) < 3.4 \text{ \AA}$  and  $(\text{O-H}\dots\text{O}) > 150^\circ$ ;  $d(\text{O}\dots\text{O}) < 4.0 \text{ \AA}$  and  $(\text{O-H}\dots\text{O}) > 120^\circ$ ;  $d(\text{O}\dots\text{O}) < 4.0 \text{ \AA}$  and  $(\text{O-H}\dots\text{O}) > 150^\circ$ .

For Table of Contents Only



## REFERENCES

1. Crowe LM. Lessons from nature: the role of sugars in anhydrobiosis. *Comp Biochem Physiol A Mol Integr Physiol*. 2002;131(3):505-513. <http://www.ncbi.nlm.nih.gov/pubmed/11867276>.
2. Ghasempour H, Gaff D, Williams R, Gianello R. Contents of sugars in leaves of drying desiccation tolerant flowering plants, particularly grasses. *Plant Growth Regul*. 1998;24(3):185-191.
3. Golovina EA, Golovin A, Hoekstra FA, Faller R. Water Replacement Hypothesis in Atomic Details: Effect of Trehalose on the Structure of Single Dehydrated POPC Bilayers. *Langmuir*. 2010;26(13):11118-11126. doi:10.1021/la100891x
4. Crowe JH. Anhydrobiosis: An Unsolved Problem with Applications in Human Welfare. *Subcell Biochem*. 2015;71:263-280. doi:10.1007/978-3-319-19060-0\_11
5. Hatley RHM, Blair JA. Stabilisation and delivery of labile materials by amorphous carbohydrates and their derivatives. *J Mol Catal B Enzym*. 1999;7(1-4):11-19. doi:10.1016/S1381-1177(99)00018-1
6. Hancock BC, Zografi G. Characteristics and significance of the amorphous state in pharmaceutical systems. *J Pharm Sci*. 1997;86(1):1-12.
7. Levine H, ed. *Amorphous Food and Pharmaceutical Systems*. Cambridge: Royal Society of Chemistry; 2002. doi:10.1039/9781847550118
8. Langer M, Höltje M, Urbanetz NA, Brandt B, Höltje H-D, Lippold BC. Investigations on the predictability of the formation of glassy solid solutions of drugs in sugar alcohols. *Int J Pharm*. 2003;252(1-2):167-179. doi:10.1016/s0378-5173(02)00647-6
9. Finch CA. Encapsulation and controlled release of food ingredients, ACS symposium series no. 590. Edited by S. J. Risch and G. A. Reineccius. American Chemical Society, Washington, 1995. pp. vii + 214, price: US\$64.95. ISBN 0-8412-3164-8. *Polym Int*. 1996;39(4):345-346. doi:10.1002/pi.1996.210390411
10. Levine H, Slade L. Another View of Trehalose for Drying and Stabilizing Biological Materials. *BioPharm*. 1992;5:36.
11. Chang B, Beauvais R, Dong A, Carpenter J. Physical Factors Affecting the Storage Stability of Freeze-Dried Interleukin-1 Receptor Antagonist: Glass Transition and Protein Conformation. *Arch Biochem Biophys*. 1996;331(2):249-258.
12. Shallenberger R. Intrinsic Chemistry of Fructose. *Pure Appl Chem*. 1978.
13. Yaylayan VA, Ismail AA, Mandeville S. Quantitative determination of the effect of pH and temperature on the keto form of d-fructose by FT IR spectroscopy. *Carbohydr Res*. 1993;248:355-360. doi:10.1016/0008-6215(93)84141-R
14. Broido A, Houminer Y, Patai S. Pyrolytic reactions carbohydrates Part I Mutarotation molten D-glucose. *J Chem Soc B Phys Org*. 1966;5:411-414.
15. Wlodarczyk P, Paluch M, Grzybowski A, et al. Mechanism of mutarotation in

- supercooled liquid phase: Studies on L-sorbose. *J Chem Phys.* 2012;137(12):124504.
16. Wlodarczyk P, Kaminski K, Paluch M, Ziolo J. Mutarotation ind-Fructose Melt Monitored by Dielectric Spectroscopy. *J Phys Chem B.* 2009;113(13):4379-4383.
  17. Dincer T, Parkinson G, Rohl A, Ogden M. Crystallisation of  $\alpha$ -lactose monohydrate from dimethyl sulfoxide (DMSO) solutions: influence of  $\beta$ -lactose. *J Cryst Growth.* 1999;205(3):368-374.
  18. Dubrunfaut M. Sur quelques phénomènes rotatoires et sur quelques propriétés des sucres. *Ann Chim Phys.* 1846;3(18):99-107.
  19. Dujardin N, Dudognon E, Willart JF, et al. Solid state mutarotation of glucose. *J Phys Chem B.* 2011;115(7):1698-1705. doi:10.1021/jp109382j
  20. Silva A, Silva Ec, Silva Co. A theoretical study of glucose mutarotation in aqueous solution. *Carbohydr Res.* 2006;341:1029-1040.
  21. Kabayama M, Patterson D, Piche L. The thermodynamics of mutarotation of some sugars .1. measurement of the heat of mutarotation by microcalorimetry. *Can J Chem Can Chim.* 1958;36(3):557-562.
  22. Kossack W, Kipnusu W, Dulski M, et al. The kinetics of mutarotation in L-fucose as monitored by dielectric and infrared spectroscopy. *J Chem Phys.* 2014;140(21):215101.
  23. Wolnica K, Dulski M, Kaminska E, et al. Unexpected Crossover in the kinetics of mutarotation in the supercooled region: the role of H-bonds. *Sci Rep.* 2018;8(1):5312.
  24. Wlodarczyk P, Paluch M, Wlodarczyk A, Hyra M. A mutarotation mechanism based on dual proton exchange in the amorphous d-glucose. *Phys Chem Chem Phys.* 2014;16(10):4694-4698.
  25. Lefort R, Caron V, Willart J-F, Descamps M. Mutarotational kinetics and glass transition of lactose. *Solid State Commun.* 2006;140(7-8):329-334. doi:10.1016/j.ssc.2006.09.003
  26. Tombari E, Ferrari C, Salvetti G, Johari G. Spontaneous liquifaction of isomerizable molecular crystals. *J Chem Phys.* 2007.
  27. Einfal T, Planinšek O, Hrovat K. Methods of amorphization and investigation of the amorphous state. *Acta Pharm.* 2013;63(3):305-334. doi:10.2478/acph-2013-0026
  28. Debenedetti PG, Stillinger FH. Supercooled liquids and the glass transition. *Nature.* 2001;410(6825):259-267. doi:10.1038/35065704
  29. Ediger MD, Angell CA, Nagel SR. Supercooled Liquids and Glasses. *J Phys Chem.* 1996;100(31):13200-13212. doi:10.1021/jp953538d
  30. Balaz P, Achimovicova M, Balaz M, et al. Hallmarks of mechanochemistry: from nanoparticles to technology. *Chem Soc Rev.* 2013;42(18):7571-7637.
  31. Takacs L. The historical development of mechanochemistry. *Chem Soc Rev.* 2013;42(18):7649-7659.
  32. Suryanarayana C. *Mechanical Alloying And Milling.* Marcel Dekker Incorporated;

- 2004.
33. Tang X, Pikal MJ. Design of freeze-drying processes for pharmaceuticals: practical advice. *Pharm Res.* 2004;21(2):191-200. <http://www.ncbi.nlm.nih.gov/pubmed/15032301>.
  34. Broadhead J, Edmond Rouan SK, Rhodes CT. The spray drying of pharmaceuticals. *Drug Dev Ind Pharm.* 1992;18(11-12):1169-1206. doi:10.3109/03639049209046327
  35. Kaminski K, Kaminska E, Wlodarczyk P, et al. Dielectric studies on mobility of the glycosidic linkage in seven disaccharides. *J Phys Chem B.* 2008;112(40):12816-12823. doi:10.1021/jp804240a
  36. Jeffrey GA, Wood RA, Pfeffer PE, Hicks KB. Crystal structure and solid-state NMR analysis of lactulose. *J Am Chem Soc.* 1983;105(8):2128-2133. doi:10.1021/ja00346a005
  37. Ngoni F, Willart J-F, Cuello G, Jimenez-Ruiz M, Affouard F. Lactulose: A Model System to Investigate Solid State Amorphization Induced by Milling. *J Pharm Sci.* September 2018. doi:10.1016/j.xphs.2018.09.013
  38. PERLIN AS, DU PENHOAT PH, ISBELL HS. Carbon-13 and Hydroxyl Proton NMR Spectra of Ketoses. In: ; 1973:39-50. doi:10.1021/ba-1971-0117.ch003
  39. Pfeffer PE, Hicks KB, Earl WL. Solid-state structures of keto-disaccharides as probed by <sup>13</sup>C cross-polarization, "magic-angle" spinning n.m.r. spectroscopy. *Carbohydr Res.* 1983;111(2):181-194. doi:10.1016/0008-6215(83)88304-9
  40. Todorov IT, Smith W, Trachenko K, Dove MT. DL\_POLY\_3: new dimensions in molecular dynamics simulations via massive parallelism. *J Mater Chem.* 2006;16(20):1911. doi:10.1039/b517931a
  41. Jorgensen WL, Maxwell DS, Tirado-Rives J. Development and Testing of the OLPS All-Atom Force Field on Conformational Energetics and Properties of Organic Liquids. *J Am Chem Soc.* 1996;118(15):11225-11236. doi:10.1021/ja9621760
  42. Kaminski GA, Friesner RA, Tirado-Rives J, Jorgensen WL. Evaluation and reparametrization of the OPLS-AA force field for proteins via comparison with accurate quantum chemical calculations on peptides. *J Phys Chem B.* 2001;105(28):6474-6487. doi:10.1021/jp003919d
  43. Damm W, Frontera A, Tirado-Rives J, Jorgensen WL. OPLS all-atom force field for carbohydrates. *J Comput Chem.* 1997;18(16):1955-1970. doi:10.1002/(SICI)1096-987X(199712)18:16<1955::AID-JCC1>3.3.CO;2-A
  44. Kony D, Damm W, Stoll S, Van Gunsteren WF. An improved OPLS-AA force field for carbohydrates. *J Comput Chem.* 2002;23(15):1416-1429. doi:10.1002/jcc.10139
  45. Caleman C, van Maaren PJ, Hong M, Hub JS, Costa LT, van der Spoel D. Force Field Benchmark of Organic Liquids: Density, Enthalpy of Vaporization, Heat Capacities, Surface Tension, Isothermal Compressibility, Volumetric Expansion Coefficient, and Dielectric Constant. *J Chem Theory Comput.* 2012;8(1):61-74. doi:10.1021/ct200731v
  46. Roberts CJ, Debenedetti PG. Structure and Dynamics in Concentrated, Amorphous

- Carbohydrate–Water Systems by Molecular Dynamics Simulation. *J Phys Chem B*. 1999;103(34):7308-7318. doi:10.1021/jp9911548
47. Lerbret A, Bordat P, Affouard F, Descamps M, Migliardo F. How Homogeneous Are the Trehalose, Maltose, and Sucrose Water Solutions? An Insight from Molecular Dynamics Simulations. *J Phys Chem B*. 2005;109(21):11046-11057. doi:10.1021/jp0468657
  48. Ngonu F, Cuello G, Jimenez-Ruiz M, et al. Morphological and structural properties of amorphous lactulose studied by scanning electron microscopy, polarised neutron scattering, and molecular dynamics simulations. *Mol Pharm*. 2019.
  49. Mayer J, Conrad J, Klaiber I, Lutz-Wahl S, Beifuss U, Fischer L. Enzymatic production and complete nuclear magnetic resonance assignment of the sugar lactulose. *J Agric Food Chem*. 2004;52(23):6983-6990. doi:10.1021/jf048912y
  50. Willart JF, Caron V, Lefort R, Danede F, Prevost D, Descamps M. Athermal character of the solid state amorphization of lactose induced by ball milling. *Solid State Commun*. 2004;132(10):693-696.
  51. Dujardin N, Willart JF, Dudognon E, et al. Solid state vitrification of crystalline  $\alpha$  and  $\beta$ -D-glucose by mechanical milling. *Solid State Commun*. 2008;148(1-2):78-82. doi:10.1016/j.ssc.2008.07.002
  52. Salah AM. Effets du broyage mécanique sur l'état physique des matériaux pharmaceutiques vitreux. *PhD Thesis*. 2015.
  53. Miller DP, de Pablo JJ. Calorimetric solution properties of simple saccharides and their significance for the stabilization of biological structure and function. *J Phys Chem B*. 2000;104(37):8876-8883. doi:10.1021/Jp000807d
  54. Wojnarowska Z, Włodarczyk P, Kaminski K, Grzybowska K, Hawelek L, Paluch M. On the kinetics of tautomerism in drugs: New application of broadband dielectric spectroscopy. *J Chem Phys*. 2010;133(9):094507. doi:10.1063/1.3475688
  55. Śmiszek-Lindert WE, Kamińska E, Minecka A, et al. Studies on dynamics and isomerism in supercooled photochromic compound Aberchrome 670 with the use of different experimental techniques. *Phys Chem Chem Phys*. 2018;20(26):18009-18019. doi:10.1039/C8CP02993H
  56. Zhou H, Xue C, Weis P, et al. Photoswitching of glass transition temperatures of azobenzene-containing polymers induces reversible solid-to-liquid transitions. *Nat Chem*. 2017;9(2):145-151. doi:10.1038/nchem.2625
  57. Lerbret A, Affouard F. Molecular Packing, Hydrogen Bonding, and Fast Dynamics in Lysozyme/Trehalose/Glycerol and Trehalose/Glycerol Glasses at Low Hydration. *J Phys Chem B*. 2017;121(40):9437-9451. doi:10.1021/acs.jpcb.7b07082
  58. Averett D, Cicerone MT, Douglas JF, de Pablo JJ. Fast relaxation and elasticity-related properties of trehalose-glycerol mixtures. *Soft Matter*. 2012;8(18):4936. doi:10.1039/c2sm25095k
  59. Soldara A, Metatla N. Glass transition of polymers: Atomistic simulation versus experiments. *Phys Rev E - Stat Nonlinear, Soft Matter Phys*. 2006;74(6):1-6.

doi:10.1103/PhysRevE.74.061803

60. Gordon JM, Rouse GB, Gibbs JH, Risen WM. The composition dependence of glass transition properties. *J Chem Phys.* 1977;66(11):4971-4976. doi:10.1063/1.433798
61. Descamps M, Willart JF, Dudognon E, Caron V. Transformation of pharmaceutical compounds upon milling and comilling: The role of Tg. *J Pharm Sci.* 2007;96(5):1398-1407.
62. Mauro JC, Yue Y, Ellison AJ, Gupta PK, Allan DC. Viscosity of glass-forming liquids. *Proc Natl Acad Sci U S A.* 2009;106(47):19780-19784. doi:10.1073/pnas.0911705106
63. OLLETT A -L, PARKER R. The Viscosity of Supercooled Fructose and Its Glass Transition Temperature. *J Texture Stud.* 1990;21(3):355-362. doi:10.1111/j.1745-4603.1990.tb00484.x
64. Willart JF, Descamps M, Caron V. Direct crystal to glass transformations of trehalose induced by milling, dehydration and annealing. *AIP Conf Proc.* 2008;982:108-113. doi:10.1063/1.2897763
65. Tsukushi I, Yamamuro O, Matsuo T. Solid state amorphization of organic molecular crystals using a vibrating mill. *Solid State Commun.* 1995;94(12):1013-1018. doi:10.1016/0038-1098(95)00161-1